Molecular Cell
Article

S. pombe LSD1 Homologs Regulate Heterochromatin Propagation and Euchromatic Gene Transcription

Fei Lan,[1] Mikel Zaratiegui,[2,4] Judit Villén,[3,4] Matthew W. Vaughn,[2,4] André Verdel,[3,5] Maite Huarte,[1] Yujiang Shi,[1,6] Steven P. Gygi,[3] Danesh Moazed,[3] Robert A. Martienssen,[2] and Yang Shi[1,*]
[1] Department of Pathology, Harvard Medical School, 77 Avenue Louis Pasteur, Boston, MA 02115, USA
[2] Cold Spring Harbor Laboratory, 1 Bungtown Road, Cold Spring Harbor, NY 11724, USA
[3] Department of Cell Biology, Harvard Medical School, 240 Longwood Avenue, Boston, MA 02115, USA
[4] These authors contributed equally to this work.
[5] Present address: Institut National de la Santé et de la Recherche Médicale, U823, Institut Albert Bonniot, Université Joseph Fourier, F-38700 Grenoble, France.
[6] Present address: Division of Endocrinology, Diabetes, and Hypertension, Department of Medicine and BCMP, Brigham and Women's Hospital and Harvard Medical School, 221 Longwood Avenue, Boston, MA 02115, USA.
*Correspondence: yshi@hms.harvard.edu
DOI 10.1016/j.molcel.2007.02.023

SUMMARY

LSD1 represses and activates transcription by demethylating histone H3K4me and H3K9me, respectively. Genetic ablation of the *S. pombe* homologs, *splsd1* and *splsd2*, resulted in slow growth and lethality, respectively, underscoring their physiological importance. spLsd1 and spLsd2 form a stable protein complex, which exhibits demethylase activity toward methylated H3K9 in vitro. Both proteins were associated with the heterochromatin boundary regions and euchromatic gene promoters. Loss of spLsd1 resulted in increased H3K9 methylation accompanied by reduced euchromatic gene transcription and heterochromatin propagation. Removal of the H3K9 methylase Clr4 partially suppressed the slow growth phenotype of *splsd1Δ*. Conversely, catalytically inactivating point mutations in the *splsd1* and *splsd2* genes partially mimicked the growth and heterochromatin propagation phenotypes. Taken together, these findings suggest the importance of both enzymatic and nonenzymatic roles of spLsd1 in regulating heterochromatin propagation and euchromatic transcription and also suggest that misregulation of spLsd1/2 is likely to impact the epigenetic state of the cell.

INTRODUCTION

Histone N-terminal tails are subject to multiple posttranslational modifications including methylation, which occurs on both lysine (K) and arginine (R) residues. A number of histone lysine residues are methylated, including histones H3K4, 9, 27, 36, and 79 as well as histone H4K20. Methylation at these sites is associated with distinct chromatin structure and promoter activities (Kouzarides, 2002; Fischle et al., 2003; Margueron et al., 2005; Lachner et al., 2004; Martin and Zhang, 2005). For instance, methylation of H3K4 is associated with active transcription, while methylation of H3K9 is linked to transcriptional repression and heterochromatin. Lysine residues can be mono-, di-, and trimethylated, and these different methylation states may also play important roles in the regulation of chromatin structure and gene transcription (Bannister and Kouzarides, 2004). Furthermore, depending on the location, the same methylation event may have different functional outcomes. Specifically, the repressive H3K9 methylation, when occurring within the body of the gene, has been shown to positively regulate transcriptional elongation (Vakoc et al., 2005). Thus, the site and the extent of methylation, as well as the location where methylation occurs at the gene locus, can all impact the functional outcome, attesting to the complexity of histone methylation in chromatin regulation.

Recent studies have shown that histone methylation is reversible by demethylases. LSD1, which is evolutionarily conserved from *S. pombe* to human, represses transcription via demethylation of H3K4me (Shi et al., 2004). The numbers of LSD1-related genes vary in different species. The *Arabidopsis* has four while both *S. pombe* and human have two LSD1-related genes (Shi et al., 2004). LSD1-mediated repression in vivo requires the associated protein Co-REST, which is a SANT domain-containing molecule (Shi et al., 2005; Lee et al., 2005). Co-REST stabilizes LSD1 (Shi et al., 2005) and provides LSD1 access to nucleosomal substrates via interactions with LSD1 (Lee et al., 2005; Shi et al., 2005), as well as contacts with DNA (Yang et al., 2006). In contrast, in the presence of the androgen receptor (AR), LSD1 is associated with active transcription and demethylation of H3K9me at the target promoters (Metzger et al., 2005). These findings demonstrate that protein-protein interactions play an important role in the regulation of the activity and substrate specificity of LSD1.

Histone methylation is associated with important biological processes, including DNA damage response and heterochromatin formation (Lehnertz et al., 2003; Peters et al., 2001; Sanders et al., 2004). In the fission yeast *S. pombe*, heterochromatin is present at a number of different genomic locales, including centromere, telomere, and the mating type loci (Grewal, 2000; Pidoux and Allshire, 2004). In the mating type and centromere loci, heterochromatin assembly has been shown to be initiated by siRNAs and requires the RNAi effector complex RITS and the RNAi machinery (Hall et al., 2002; Verdel et al., 2004; Volpe et al., 2002). This is followed by recruitment of the H3K9 histone methylase Clr4, the *S. pombe* homolog of Suv39H (Ivanova et al., 1998; Rea et al., 2000). Heterochromatin propagation is believed to involve the *S. pombe* HP1 homolog Swi6, which binds methylated H3K9 as well as the methylase Clr4 (Nakayama et al., 2001). In general, *S. pombe* heterochromatin is characterized by H3K9 hypermethylation and H3K4 hypomethylation, but the heterochromatin boundaries are associated with hypermethylated H3K4 and hypomethylated H3K9, respectively (Noma et al., 2001). Because human LSD1 mediates demethylation of both H3K4 and H3K9 (Metzger et al., 2005; Shi et al., 2004), these findings collectively raise the question of whether *S. pombe* LSD1 homologs may play a role in regulating H3K4 and/or H3K9 methylation at heterochromatin, therefore impacting heterochromatin assembly and/or propagation.

In this report, we investigated the biological functions of LSD1 in the model organism *S. pombe*, which contains two LSD1 homologs, spLsd1 and spLsd2. Genetic ablation of *splsd1* or *splsd2* resulted in significant growth retardation or lethality, respectively, underscoring their physiological significance. Global gene expression profiling as well as genomic localization of spLsd1/2 by chromatin immunoprecipitation coupled microarray (ChIP-chip) implicated spLsd1/2 in both heterochromatin and euchromatin functions. Specifically, loss of spLsd1 resulted in a modest global increase of methylation at H3K9, but not at other lysine residues. In *splsd1Δ* cells, the increase of H3K9 methylation at the heterochromatin boundary appeared to be associated with heterochromatin expansion. ChIP-chip analysis identified spLsd1/2 at the target sites/genes, suggesting that spLsd1/2 directly regulate heterochromatin propagation and euchromatic gene transcription by antagonizing H3K9 methylation. Several lines of evidence supported this model. First, the growth phenotype was rescued specifically, albeit incompletely, by suppression of the H3K9 methylase Clr4, but not other methylases. Second, the growth and heterochromatin propagation phenotypes were mimicked partially by introduction of catalytically inactivating point mutations in the *splsd1* and *splsd2* genes. Third, recombinant spLsd1 and the spLsd1/2 complex exhibited H3K9 demethylase activity in vitro. Taken together, these findings identified critical functions of spLsd1 and spLsd2 in the regulation of heterochromatin propagation as well as transcription of a large number of euchromatic genes, in part by antagonizing H3K9 methylation through the H3K9 demethylase activity.

RESULTS

spLsd1 and spLsd2 Are Important for *S. pombe* Growth and Viability

S. pombe has two LSD1-like open reading frames (ORFs), spbc146.09c and spac23e2.02. For simplicity, we refer to these two genes as *splsd1* and *splsd2*, respectively (Figure 1A). We succeeded in knocking out *splsd1* (*splsd1Δ*) but were unable to obtain transformants for *splsd2Δ* using PCR mediated strategy, suggesting that spLsd2 was likely to be required for cell viability. We also failed to isolate *splsd2Δ* strain through sporulation of a heterozygote diploid strain. Interestingly, the $splsd1^{+/-}$ diploid cells were also defective in sporulation with only a very small fraction of the diploid cells producing viable spores, suggesting that both spLsd1 and spLsd2 may be involved in regulating *S. pombe* meiosis. Consistent with this hypothesis, the expression of both *splsd1* and *splsd2* is increased significantly during the S phase of meiosis (Mata et al., 2002). *splsd1Δ* exhibited an array of phenotypes including severely retarded growth (doubling time of 8 hr as opposed to 2.1 hr for the wild-type [WT] cells), flocculation, heterogeneity, and significant loss of viability during growth (Figures 1B and 1C). Reintroduction of WT $splsd1^{+}$ restored normal growth, indicating that the slow growth phenotype was likely to be the result of genetic inactivation of the endogenous $splsd1^{+}$ gene. Taken together, these findings identified an essential function for spLsd1 and spLsd2 in *S. pombe* growth and viability and suggested that these two proteins may have both redundant and nonredundant functions.

spLsd1 Demethylates and Antagonizes H3K9 Methylation

Human LSD1 functions as a histone demethylase that reverses H3K4 and H3K9 methylation, respectively (Metzger et al., 2005; Shi et al., 2004). We investigated whether spLsd1 and/or spLsd2 regulated *S. pombe* growth as histone demethylases, using recombinant protein purified from insect cells as well as spLsd complex purified from *S. pombe*. To purify spLsd1/2 complex, we first generated yeast strains carrying C-terminally TAP-tagged $lsd1^{+}$ and $lsd2^{+}$ genes, respectively, in place of the endogenous genes. These yeast cells were indistinguishable from the WT *S. pombe*, suggesting that the C-terminal TAP did not alter the functions of spLsd1 or spLsd2. As shown in Figure 2A, spLsd1 and spLsd2 are present in the same, stable protein complex. The core spLsd1/2 complex components included approximately stoichiometric quantity of spLsd1, spLsd2, and two PHD domain proteins (SPCC4G3.07c and SPAC30D11.08c, see Table S4 in the Supplemental Data available with this article online), which we refer to as Phf1 (*PHD finger 1*) and Phf2, respectively. Consistent with the fact that they are components of the same protein complex, the expression patterns of

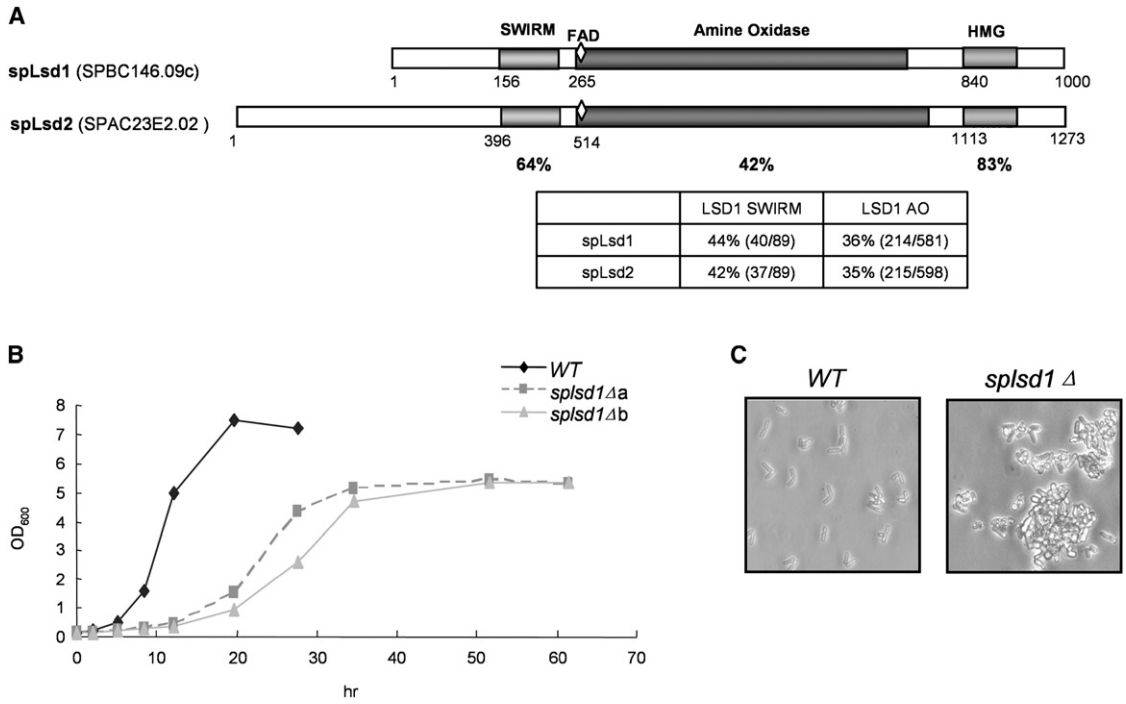

Figure 1. *S. pombe* LSD1 Homologs Regulate Cell Growth

(A) Schematic diagram of domain structures of spLsd1 and spLsd2 and sequence homology comparison with human LSD1. AO, amine oxidase.

(B) Two individual clones of *splsd1Δ* display severe growth defects.

(C) Microscopic images of WT and *splsd1Δ*; note that *splsd1Δ* displays flocculation and irregular cell shapes.

Phf1 and Phf2 during meiosis were found to be similar to that of spLsd1 and spLsd2 (Mata et al., 2002). Furthermore, we were unable to obtain the knockout strains for them either by the PCR-mediated strategy or through heterozygote sporulation, suggesting that, similar to spLsd1 and spLsd2, Phf1 and Phf2 were also likely to be required for cell viability and meiosis. The precise roles of Phf1 and Phf2 remain to be investigated.

We next assayed the recombinant spLsd1 and the purified spLsd1 complex for histone demethylase activities. Bulk histones were methylated at H3K4 and H3K9 by the recombinant methylases Set7/9 and Clr4, respectively, in the presence of radioactively labeled [^{3}H]methyl-methionine. The demethylation reactions were monitored by the production of the radioactively labeled formaldehyde, which has shown to be a demethylation reaction product (Shi et al., 2004). As shown in Figure 2B, WT, but not the predicted, catalytically inactive spLsd1 point mutant (illustrated in the top panel of Figure 2B), demethylated H3K9, but not H3K4 on the bulk histones. Likewise, the spLsd1 protein complex also demethylated H3K9, but not H3K4. Importantly, the spLsd1 complex purified from the strain carrying the mutations predicted to inactivate both spLsd1 and spLsd2 (spLsd1/2mm) also failed to demethylate H3K9 (Figure 2B). Although the Clr4-labeled histone substrates may include both radioactive H3K9me2 and H3K9me3, the released formaldehyde was likely to have resulted from demethylation of H3K9me2 due to the inherent chemistry of LSD1 family of demethylases (Shi et al., 2004). Consistently, analysis of bulk histones isolated from the WT and the *splsd1Δ* strains also showed loss of spLsd1 associated with a mild but significant increase in the total H3K9me2 level without overt effects on the levels of H3K4me2, H3K36me2, or H4K20me2 (Figure S1).

We next carried out genetic suppression experiments to determine whether ablation of an H3K9 methylase may suppress the growth phenotype associated with the *splsd1Δ* cells. Consistent with the biochemical data, deletion of *clr4*, which encodes the main, if not the only, *S. pombe* H3K9 methylase (Cam et al., 2005), partially suppressed the growth retardation phenotype (Figure 2C, doubling time of ~5 hr). In contrast, deletion of the other methylase genes including *set1* (H3K4) and *set2* (H3K36) enhanced the growth retardation defect, suggesting possible collaborations between spLsd1 and these methylases (Figure 2C). Deletion of the H4K20 methylase gene *set9* suppressed the growth phenotype slightly, and the significance of this remained unclear. As controls, we found that growth of the individual methylase knockout strains used in the suppression experiments was comparable to that of the WT *S. pombe* (data not shown). Taken together, these findings suggested that spLsd1 functioned in part by antagonizing Clr4, which mediates H3K9 methylation in *S. pombe*. However, the weak suppression also suggested spLsd1 functions that were independent of antagonizing H3K9 methylation.

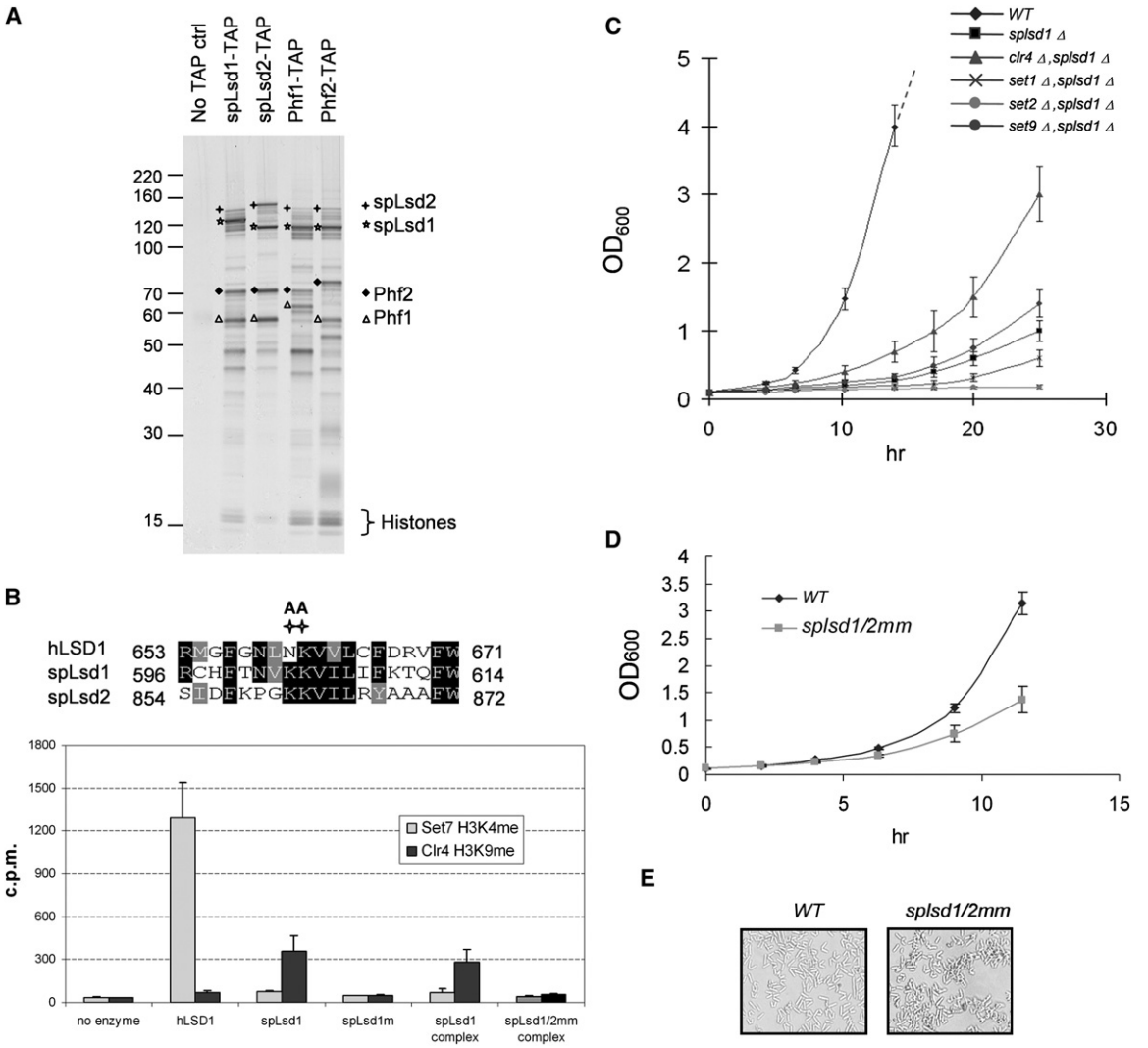

Figure 2. spLsd1 Demethylates H3K9me and Catalytically Important Lysine Residues Are Required for Full spLsd1/2 Function

(A) TAP purification of spLsd1 and spLsd2 complexes. TAP purification of spLsd1 identified spLsd2 and two PHD finger proteins. Subsequently, new components of the spLsd1 complex were TAP tagged at the C terminus and subjected to TAP purification. Again, the same four core components of the complex have been identified by MS-MS. The corresponding bands from individual purification have been marked as star for spLsd1, cross for spLsd2, open triangle for Phf1, and solid diamond for Phf2. Note that all four histone species were found in the purification, suggesting that spLsd1/2 complex is tightly associated with chromatin. A full list of copurified protein components can be found in Table S4.

(B) (Top panel) Sequence alignment of human LSD1 and spLsd1/2 surrounding hLSD1 lysine 661, which is critical for demethylation (Lee et al., 2005) and is conserved in both spLsd1 and spLsd2. There is also an additional lysine next to this conserved lysine that appears to be specific to spLsd1/2. Both lysine residues were mutated to alanine (A), and mutant strains carrying either mutated *splsd1* or *splsd2* singly (*splsd1m* and *splsd2m*) or together (*splsd1/2mm*) were generated. (Bottom panel) Histone H3K9me demethylase activities of recombinant Flag-spLsd1, purified from baculovirus-infected Sf9 cells, and spLsd1 complex purified from *S. pombe*. The assay results were shown with the average of three independent reactions with standard deviations.

(C) Growth curves of double knockout of *splsd1* in combination with four different methylase genes, respectively. Suppression of *clr4* in *splsd1Δ* partially restored growth.

(D and E) Growth curves and microscopic images of WT and the double catalytically inactive point mutant, *splsd1/2mm*. *splsd1/2mm* displays irregular cell shape and flocculation, as does *splsd1Δ*. It also displays growth retardation similar to that of *splsd1Δ*, albeit to a much lesser extent. Error bars in (C) and (E) represent standard deviations from three independent cultures.

To further explore the possibility that spLsd1 functioned as a histone demethylase, we analyzed the catalytic mutant strains carrying either mutated *splsd1* or *splsd2* singly (*splsd1m* and *splsd2m*), or together (*splsd1/2mm*). We found that while single gene mutants behaved like WT, the double mutant *splsd1/2mm* was mildly growth retarded but with a significantly reduced severity compared to *splsd1Δ* (Figure 2D; *splsd1/2mm* doubling time, 2.5 hr;

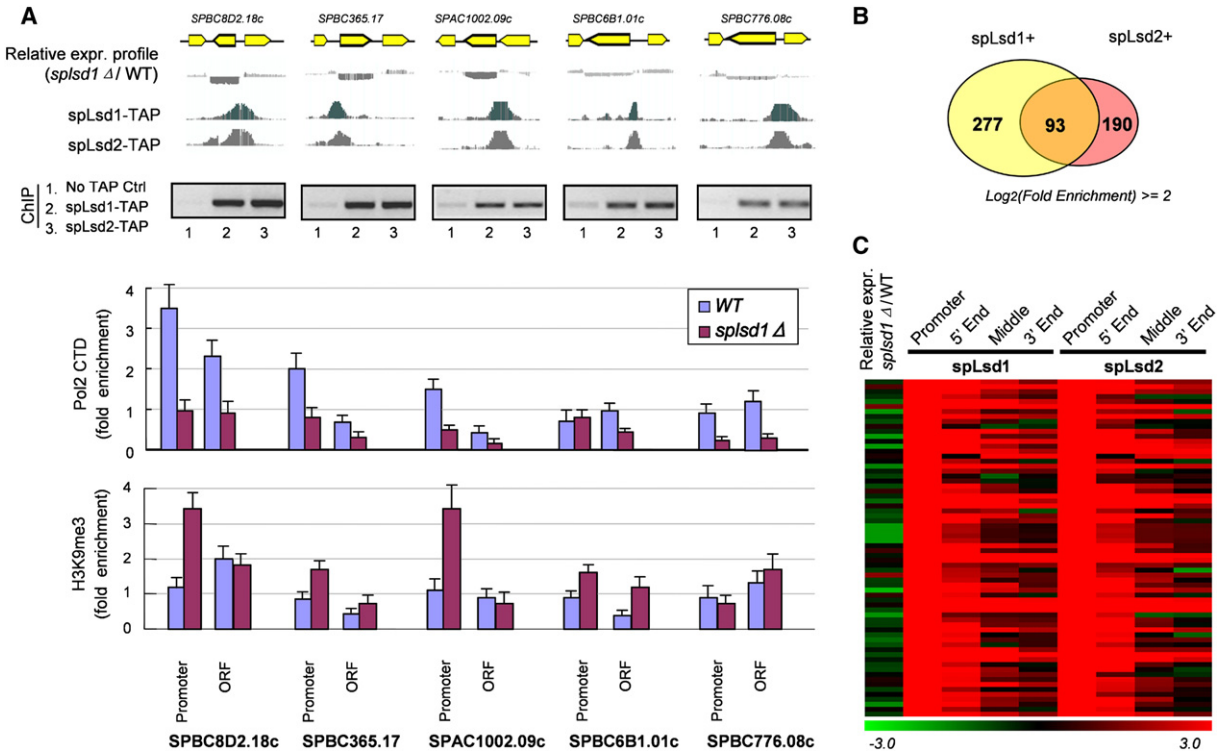

Figure 3. spLsd1 Antagonizes H3K9 Methylation and Is Required for Pol II Recruitment and Transcriptional Activation of Euchromatic Genes

(A) ChIP-chip analysis identifies spLsd1 and spLsd2 at a number of euchromatic gene promoters. Increased H3K9me3 level and reduced Pol II occupancy at the target promoters are associated with spLsd1 deletion. H3K9me3 and Pol II ChIP assays were carried out using the multiplex PCR approach (see Experimental Procedures), and the results are presented as ratios of the experimental to control PCR products (mean + SEM).

(B) Significant overlap of spLsd1 and spLsd2 target genes. A total of 560 genes exhibited spLsd1 or spLsd2 enrichment at their promoters of >4-fold of the array mean value. A total of 93 promoters were enriched for both spLsd1 and spLsd2.

(C) Microarray analysis comparing expression profiles with spLsd1/2 distribution for the 68 highest-confidence target genes. In this visualization of microarray data, the leftmost column compares *splsd1Δ* expression to that of WT cells, while the other columns show spLsd1 and spLsd2 enrichment at promoter, 5′ end, middle, and 3′ end of the genes. Green indicates decreased transcription or depletion, and red indicates enhanced transcription or enrichment. Both spLsd1 and spLsd2 are highly enriched at promoters and 5′ of the coding regions of their targets, and a majority of spLsd1/2 targets display reduced transcription upon deletion of *splsd1*.

WT, 2.1 hr; and *splsd1Δ*, 8 hr). This double mutant also displayed slight flocculation similar to that of *splsd1Δ* cells (Figure 2E). Thus, mutations that inactivate the demethylase activity partially phenocopied *splsd1Δ*, suggesting that the biological function of spLsd1/2 was associated with both the demethylase activity and the nonenzymatic roles of spLsd1/2.

Genomic Locations of spLsd1 and spLsd2 and Alteration of H3K9 Methylation Associated with the Loss of spLsd1

To further investigate the role of spLsd1/2 in regulating H3K9 methylation, we turned to the genome-wide ChIP-chip approach in order to determine whether (1) H3K9me2 (and/or H3K4me2) was altered at the genome-wide level as a result of deletion of *splsd1*, and (2) whether this alteration was correlated with spLsd1 (and/or spLsd2) occupancy at the corresponding genomic locales. ChIP-chip experiments were performed using a high-density DNA tiling array constructed based on the genome sequence of *S. pombe*. We found that spLsd1 and spLsd2 shared similar, but not identical genomic distribution patterns (Figures 3A and 4B). We found spLsd1 and spLsd2 to be present at a large number of euchromatic promoters and at the boundary regions of pericentromeric heterochromatin, suggesting that spLsd1 might antagonize H3K9 methylation at both heterochromatic boundaries and euchromatic regions. This hypothesis was further explored.

When the threshold was set at $\log_2$Enrichment $\geq$ 2 (4-fold), we found 93 spLsd1 and spLsd2 co-occupying promoters. spLsd1 and spLsd2 also occupied 277 and 190 unique promoters, respectively (Figure 3B), consistent with the different phenotypes associated with the deletion of *splsd1* and *splsd2*. The ChIP-chip results were confirmed by individual ChIP experiments (Figure 3A and data not shown). Some of these direct targets are actively transcribing housekeeping genes, including actin and ubiquitin, as determined by genome-wide expression

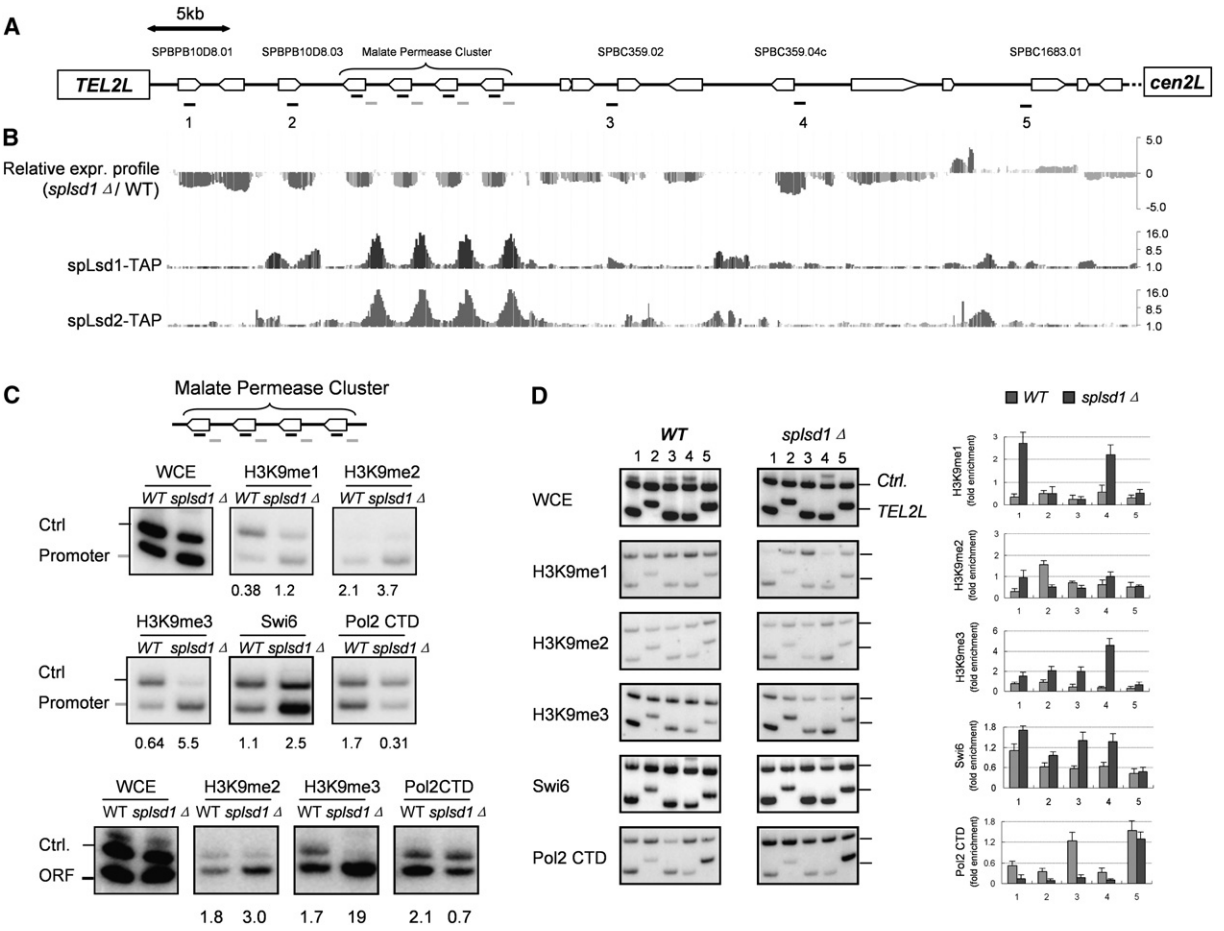

Figure 4. Loss of spLsd1 Results in Increased H3K9 Methylation and Swi6 Binding at the Subtelomere Region of the Left Arm of Chromosome 2

(A) Schematic diagram of the genomic organization of the leftmost 50 kb region of Chr2 in the Nimblegen tiling array, and positions of the primers used in ChIP experiments are indicated by short bars.

(B) Expression profiling of WT and *splsd1Δ*. Transcription in this region is found to be downregulated in the *splsd1* deletion mutant. Enrichment of spLsd1 and spLsd2 from ChIP-chip assays is also shown.

(C) ChIP analysis of H3K9 methylation and Swi6 binding at the malate gene cluster. Note that H3K9me3 is significantly increased at the promoters and ORFs, while H3K9me2 increase occurred to a lesser extent.

(D) ChIP analysis demonstrating increase of H3K9me3 and Swi6 binding at the region diagrammed in (A) in the *splsd1Δ* mutant. ChIP PCR was done using the multiplex PCR approach (see Experimental Procedures), and the results are presented as ratios of the experimental to control PCR products (mean + SEM).

profiling experiments (Table S1). Using conventional ChIP, we found that lack of spLsd1 is associated with an increased H3K9 tri-, but not dimethylation, at 4 out of the 5 target promoters examined, but not the coding regions (Figure 3A). Cluster analysis found ~60% of the spLsd1/2 common targets to be downregulated upon *lsd1* deletion (Figure 3C), indicating spLsd1 may play a direct role in active transcription. Consistent with this view, we observed reduction of RNA polymerase II (Pol II) occupancy at the target gene loci in the absence of spLsd1 (Figure 3A). Twenty-five of the spLsd1/2 target genes were represented on the spotted microarrays used by Hansen et al. (2005), and six of them were upregulated more than 1.5× in *clr4-681* cells (Table S2). These data suggested that spLsd1 activates transcription of target genes by preventing trimethylation of histone H3K9 and/or by facilitating recruitment of an H3K9 tridemethylase.

We also investigated spLsd1 and spLsd2 function at the subtelomeric region of *TEL2L* including a cluster of malate permease genes (Figure 4A). Both proteins were highly enriched at the promoters of the malate permease genes and mildly enriched at the surrounding regions. A significantly reduced transcription was associated with the leftmost 13 ORFs of *TEL2L* including the malate permease genes in *splsd1Δ* (Figure 4B). Using conventional ChIP, a significant increase of H3K9me1, 2, and 3 at the promoters of the malate permease genes was also detected in *splsd1Δ* (Figure 4C). This increase was accompanied by ~2-fold

increase of Swi6 binding at the promoter regions, and a significant reduction of Pol II occupancy at both the promoter and coding regions (Figure 4C). Interestingly, we did not detect a similar regulation of H3K9me or any enrichment of spLsd1 or spLsd2 at the other subtelomeric regions including *TEL1R* and *TEL1L* (data not shown). Finally, we also found increased H3K9me3, but not H3K9me1/2, and increased Swi6 binding in the region surrounding the malate permease genes in *splsd1Δ* (Figure 4D, lanes 1–4). Consistently, reduced Pol II occupancies were also observed (Figure 4D, lanes 1–4). Collectively, these findings suggested that reduced transcription in the subtelomeric region of *TEL2L* might be due to a direct action of spLsd1/2 at this euchromatic region.

In addition to direct targets of spLsd1 and spLsd2, expression analysis revealed a number of indirect targets, whose expression was either elevated or reduced in *splsd1Δ* but which did not bind either spLsd1 or spLsd2. Interestingly, of the 67 genes upregulated by more than 1.5× in *splsd1Δ*, 46 were also upregulated in Δ*clr3 clr6-1* double mutant strains (Hansen et al., 2005) (Table S3). These genes included noncoding RNA from the *dg* and *dh* centromeric repeats, which were investigated further.

spLsd1 and spLsd2 Regulate Pericentromeric Heterochromatin Propagation

Our ChIP-chip analysis detected spLsd1 and spLsd2 at the heterochromatin boundary regions flanking each of the three centromeres (Figure 5A and Figure S2). Specifically, spLsd1/2 was localized to the *imr* repeats flanking both ends of the centromeric *dg-dh* repeats but was absent within the silent heterochromatin. These regions contain the tRNA genes, which have been previously reported to act as boundary elements for heterochromatin (Noma et al., 2006; Scott et al., 2006).

The spLsd1 and spLsd2 localization patterns at the heterochromatic regions prompted us to investigate the possibility that spLsd1 and spLsd2 may function together with the boundary elements to regulate heterochromatin propagation. Consistent with this model, the histone methylation profiling showed that the heterochromatin epigenetic marker H3K9me2 was shifted toward the *imr* region at all three centromeres in *splsd1Δ* (Figure 5A and Figure S2). That is, H3K9me2 was reduced over the *dg* and *dh* heterochromatic repeats but spread over the *imr* repeats. Similar H3K9me2 spreading has been shown in an *imr* $tRNA^{Ala}\Delta$ mutant, in which the barrier is impaired (Scott et al., 2006). Interestingly, this *imr* $tRNA^{Ala}\Delta$ also displays meiotic chromosome segregation defects, and in combination with the depletion of another *imr* $tRNA^{Glu}$, results in cell death (Scott et al., 2006). Thus, it is possible that growth retardation and lethality associated with the loss of spLsd1 and spLsd2, respectively, may be due in part to inappropriate regulation of heterochromatin at the centromeric regions.

We further analyzed H3K9 methylation at the heterochromatin boundaries in *splsd1Δ* by conventional ChIP. We first confirmed H3K9me2 expansion at *imr1* and *imr2* regions (Figures 5C and 5E). Interestingly, in addition to H3K9me2, we also detected a significant increase and expansion of H3K9me3, but not H3K9me1, at these regions (Figures 5C and 5E). Consistently, we also detected an elevated level of Swi6 (Figures 5C and 5E), suggesting that heterochromatin components were also spreading over the boundaries as well as H3K9me2/3. Notably, these increases correlated well with spLsd1 and spLsd2 localization at these regions, indicating that they were probably the direct consequence of the loss of spLsd1. Because trimethyl group is not a substrate of the LSD1-like enzymes due to the inherent chemistry (Shi et al., 2004), the increase of H3K9me3 at these regions may be a result of increased H3K9me2. We speculate that upon spLsd1 loss, H3K9me2 demethylation cannot be effectively executed at the heterochromatin boundaries, thus resulting in the accumulation of H3K9me2 and further conversion into H3K9me3 and subsequent Swi6 recruitment. The abnormal expansion of the heterochromatin domain in *splsd1Δ* suggested that spLsd1 may function as a boundary factor by regulating H3K9 methylation levels.

In contrast to the increased H3K9me at the boundaries, the H3K9me2 level in *dg* and *dh* repeats was reduced (Figure 5A and Figure S2). This reduction was also confirmed by conventional ChIP (Figure S3A). Transcripts from this region were elevated (Figures S3C and S3D), but the mature 23 nt small interfering RNA levels remained unchanged, suggesting that these transcripts were elevated at the transcriptional rather than the posttranscriptional level. Similar upregulation of these transcripts was previously observed in *clr3Δclr6-1* double mutant strains (Hansen et al., 2005).

Functional Analysis of Heterochromatin Expansion at the *MAT* Locus in the *splsd1Δ* Strain

We further investigated a potential role of spLsd1 in heterochromatin, taking advantage of a strain that carries an *Ade6*$^+$ reporter inserted into the boundary region between *REII* and *IR-L* at the *MAT* locus (Figure 6A; Shankaranarayana et al., 2003). This region is subject to weak silencing in WT cells, which results in a low level of expression of the *ade6* gene, and when cultured in low adenine medium, the parental strain produces a heterogeneous population of white and red colonies. Red color indicates silencing of the *ade6* gene, while white color indicates expression of the *ade6* gene and thus a loss of heterochromatin-mediated gene silencing. The *splsd1Δ* strain has a very slow growth rate, making it virtually impossible to carry out the *Ade6* reporter assay in this knockout strain. To circumvent this problem, we asked whether a reduction of spLsd1 or spLsd2 protein levels might affect heterochromatin propagation. In the *ade6*$^+$ indicator strain, we replaced the endogenous *splsd1* or *splsd2* promoters with the *nmt81* promoter, which allowed for a significantly reduced level of spLsd1 or spLsd2 expression (Figure 6B). Interestingly, the strains with low levels of spLsd1 or spLsd2 showed a decrease in *ade6* gene expression as reflected by the appearance of more red colonies (Figure 6B), suggesting an

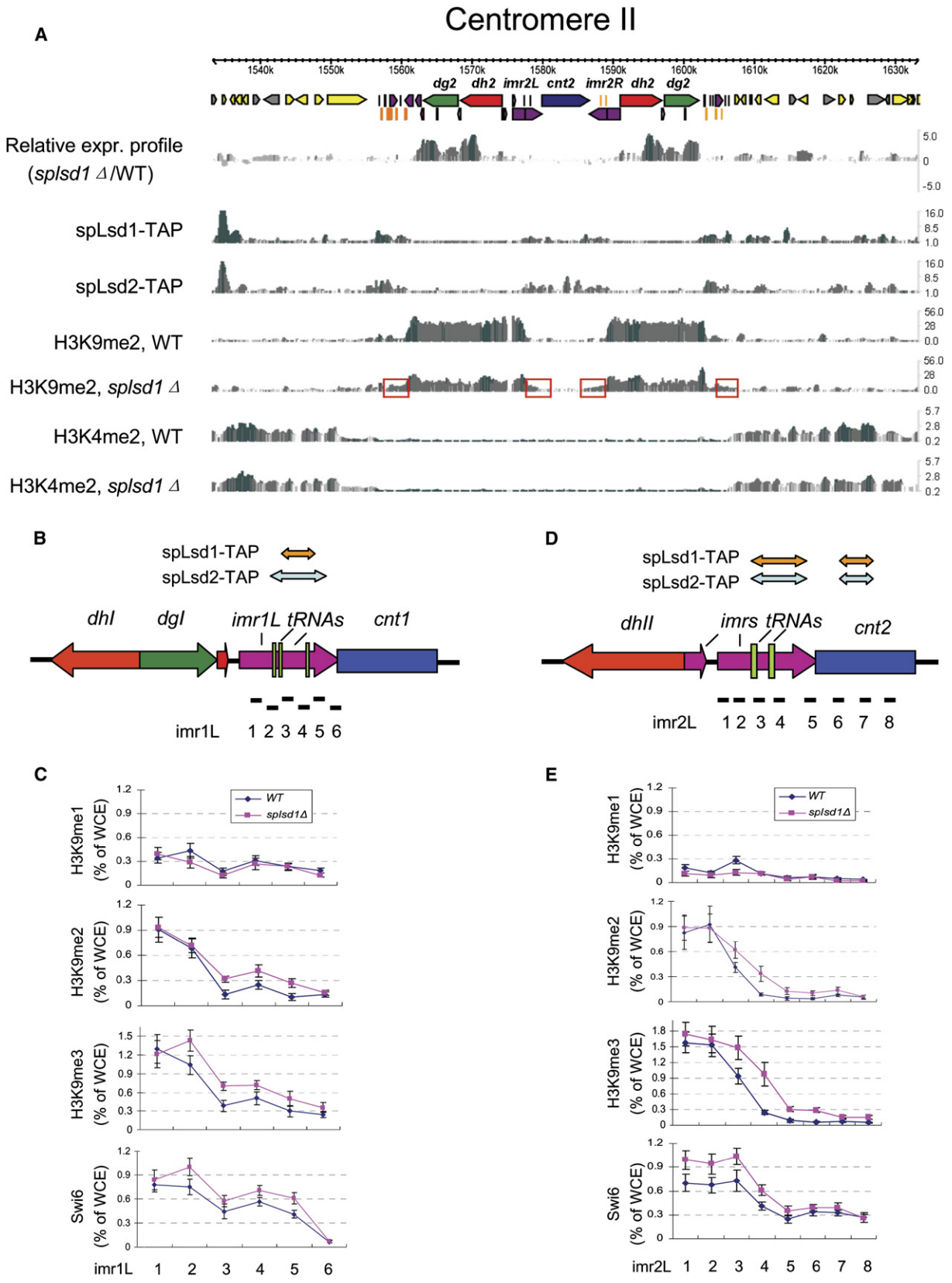
A
Centromere II
1540k
1550k
1560k
1570k
1580k
1590k
1600k
1610k
1620k
1630k
dg2 dh2 imr2L cnt2 imr2R dh2 dg2
Relative expr. profile (splsd1 Δ/WT)
spLsd1-TAP
spLsd2-TAP
H3K9me2, WT
H3K9me2, splsd1 Δ
H3K4me2, WT
H3K4me2, splsd1 Δ
B
spLsd1-TAP
spLsd2-TAP
dhI dgI imr1L tRNAs cnt1
imr1L 1 2 3 4 5 6
D
spLsd1-TAP
spLsd2-TAP
dhII imrs tRNAs cnt2
imr2L 1 2 3 4 5 6 7 8
C
H3K9me1 (% of WCE)
H3K9me2 (% of WCE)
H3K9me3 (% of WCE)
Swi6 (% of WCE)
WT
splsd1Δ
imr1L 1 2 3 4 5 6
E
H3K9me1 (% of WCE)
H3K9me2 (% of WCE)
H3K9me3 (% of WCE)
Swi6 (% of WCE)
WT
splsd1Δ
imr2L 1 2 3 4 5 6 7 8

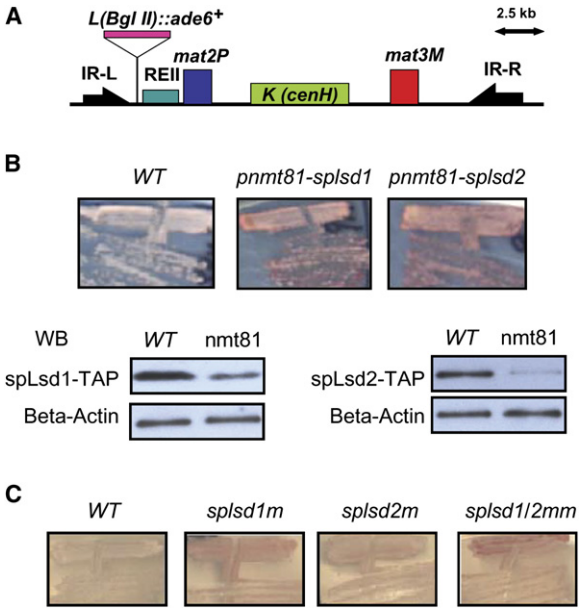

Figure 6. spLsd1 and spLsd2 Regulate Heterochromatin Silencing at *IR-L* of the *MAT* Locus

(A) Schematic diagram of the mating-type region and the position of integrated *ade6* reporter.

(B) Endogenous promoters of spLsd1 and spLsd2 were replaced by the inducible *nmt81* promoter. Cells were streaked on the YE plates and incubated at 30°C for 3 days. The levels of spLsd1 and spLsd2 were monitored by western analysis using an antibody that recognizes the C-terminal TAP tag. Note that reduced levels of spLsd1 and spLsd2 resulted in increased silencing at the *IR-L* boundary element, as reflected by the red color of the cells.

(C) Same analysis as (B) of the point mutants carrying catalytically inactivating mutations in spLsd1 and spLsd2. The mutants displayed increased silencing at the *IR-L* boundary element, and the silencing effect was additive in cells carrying mutations in both *splsd1* and *splsd2* (*splsd1/2mm*).

increase in silencing of the *ade6*$^+$ gene. Consistent with this, conventional ChIP detected elevated H3K9me3 and Swi6 binding at the same *IR-L* region in *splsd1Δ* and ChIP-chip also found spLsd1/2 localization at both ends of the *MAT* locus (data not shown).

We next asked whether this gain of silencing was dependent on the histone demethylase activity of spLsd1 and spLsd2. To address this issue, the *ade6*$^+$ indicator strains carrying the catalytically inactive alleles of *splsd1m* and *splsd2m* either singly or together were tested in the silencing assay. As shown in Figure 6C, mutations of the catalytically important lysine residues in spLsd1 (*splsd1m*) resulted in an enhanced silencing of the *ade6*$^+$ reporter. Although strains carrying *splsd2m* did not display significant alterations of the reporter level, strains carrying mutations in both *splsd1* and *splsd2* (*splsd1/2mm)* further enhanced silencing, suggesting that spLsd1 and spLsd2 collaboratively regulate heterochromatin boundaries through their demethylase activities. However, the gain of silencing in *splsd1/2mm* was less than that in the strains with reduced levels of spLsd1 or spLsd2, indicating that the enzymatic independent functions of spLsd1 and spLsd2 are involved in their boundary activities as well. Taken together, our analysis at the centromere and the *MAT* locus suggested that spLsd1 and spLsd2 function to prevent heterochromatin propagation into adjacent regions, and this function is at least in part if not all through H3K9 demethylation.

DISCUSSION

We have provided a number of insights into functions of LSD1-like demethylases. Importantly, our findings showed that spLsd1 is an H3K9 demethylase, which regulates heterochromatin in fission yeast by preventing spreading of histone H3K9 methylation at heterochromatin boundaries. We demonstrated that spLsd1 also functioned to activate target euchromatic gene transcription, by antagonizing euchromatic H3K9 methylation and by facilitating Pol II recruitment. Interestingly, the H3K9me3 level increase is more significant than that of H3K9me2 at its target sites/promoters in the *lsd1Δ* strain, suggesting that spLsd1 functions to balance H3K9me2 and H3K9me3 levels. Our studies thus uncovered an important function for spLsd1/2 in heterochromatin barrier regulation as well as a direct transcriptional activation role for euchromatic genes.

spLsd1/2 and Heterochromatin Boundary

Heterochromatic H3K9 methylation is guided by the RNAi machinery, which recruits the histone H3K9 methylase Clr4 and the H3K9 methyl-binding protein Swi6 (Martienssen et al., 2005). Spreading of these modifications from the repeats into the reporter genes depends on readthrough transcription and "slicing" by Argonaute (Irvine et al., 2006), but mechanisms that control propagation outside the heterochromatin boundary are largely unknown. Nine

Figure 5. Heterochromatin Expansion at the *otr-imr* Boundaries in *splsd1* Deletion Cells

(A) The genomic distribution of spLsd1 and spLsd2 at the heterochromatin of centromere II is shown using Genome Browser analysis. Genes (yellow and gray), *dg* repeats (green), *dh* repeats (red), *imr* repeats (purple), and tRNA genes (orange) are indicated by different colors. H3K9me2 and H3K4me2 tracks from WT and *splsd1Δ* were also plotted, and H3K9me2 expansion at the *imr* regions is indicated by red boxes. Microarray results comparing the WT and *splsd1Δ* transcript levels are also displayed, and *dg-dh* transcripts are significantly increased in *splsd1Δ*.

(B and D) Schematic diagrams of the genomic organization of the *imr1L* regions, and positions of ChIP primers. Enrichment of spLsd1 and spLsd2 based on the ChIP-chip assays is shown by the bidirectional arrows.

(C and E) Conventional ChIP analysis showing the distributions of H3K9me1, H3K9me2, H3K9me3, and Swi6 at the heterochromatin boundaries of *imr1L* and *imr2L*. ^{32}P-CTP-labeled PCR product signals from ChIP samples of the heterochromatin locus were normalized to those from WCE, and relative percentages are shown as mean ± SEM (see Experimental Procedures).

of the 12 pericentromeric boundary regions have tRNA genes, which are required for boundary function (Scott et al., 2006). TFIIIC recognizes the B box regions in the tRNA genes (Noma et al., 2006; Scott et al., 2006). B boxes are also found outside tRNA genes within the inverted repeats that flank heterochromatin surrounding the silent mating type cassettes. Deletion of these B boxes abolishes TFIIIC recruitment, resulting in abnormal H3K9me spreading beyond the boundaries (Noma et al., 2006; Scott et al., 2006). These observations suggest that histone modifications at these boundaries are dynamically regulated and important for heterochromatin propagation. This dynamic histone methylation at the boundaries is likely to involve spLsd1/2, based on our findings that spLsd1/2 are specifically enriched at some of tRNA genes located at *imr* regions of centromeres, and that spLsd1 deletion is associated with the expansion of H3K9me2, H3K9me3, and Swi6 into the *imr* regions (Figure 5).

The observation that loss of spLsd1 causes H3K9 methylation and Swi6 spreading suggests that a physiological role of spLsd1 may be to block heterochromatin spreading at the boundary. How do spLsd1/2 carry out this function? The simplest model is that spLsd1/2 located at the heterochromatin boundaries mediate demethylation of H3K9me. This is supported by the finding that spLsd1 is an H3K9 demethylase. The inverse relationship that we have identified between spLsd1/2 binding at the boundaries and the expansion of H3K9 methylation is also consistent with this hypothesis. An enzymatic role for spLsd1/2 in this regulation is further supported by our finding that silencing of the *Ade6*$^{+}$ reporter at the *IR-L* boundary is enhanced in the spLsd1 and spLsd2 point mutant strains (Figure 6C). An alternative, but not mutually exclusive, possibility is that spLsd1/2 may restrict access of Clr4, either as a consequence of its ability to antagonize H3K9 methylation or via a yet unknown mechanism. However, it should be noted that most likely the biological roles of spLsd1/2 involve both the demethylase activity as well as enzymatic independent functions because (1) *clr4Δ* only partially suppressed the *splsd1Δ* growth phenotype, (2) the *splsd1/2* catalytically inactive double mutant strain showed only mild growth retardation, and (3) the *splsd1/2* catalytically inactive double mutant affected target gene transcription to a lesser extent than that of the deletion mutant (data not shown).

spLsd1 is required for optimal cell growth, but spLsd2 is essential for viability, suggesting important physiological functions for both proteins. Because of the lethality, it was not possible to directly investigate the role of spLsd2 in heterochromatin expansion. However, three lines of evidence are consistent with the possibility that it too is involved in this regulation. First, purification of spLsd1 and spLsd2 demonstrated that most of spLsd1 and spLsd2 in the cell are in the same biochemical complex (Figure 2A). Second, ChIP analysis showed significant colocalization of both proteins (Figure 3B). Third, reduced level of either spLsd1 or spLsd2 had a similar effect on *IR-L ade6* reporter transcription, and catalytically critical lysine mutations of spLsd1 and spLsd2 had an additive effect on the reporter expression (Figure 6).

A Role for spLsd1/2 in Activating Gene Transcription

Loss of spLsd1 is associated with a significant decrease of transcription of most euchromatic target genes identified by ChIP (Figure 3C and Table S1), suggesting an activating function for spLsd1/2. The correlation between spLsd1/2 promoter occupancy and transcript levels suggests a direct role of spLsd1/2 in mediating transcriptional activation. Significantly, spLsd1 promoter occupancy is inversely correlated with H3K9me increase, suggesting that spLsd1 antagonizes H3K9 methylation at the target promoters as well. We speculate that loss of spLsd1 resulted in an initial increase in H3K9me2 level, which is converted to H3K9me3 by a yet-to-be-identified histone methylase. The fact that the increase in H3K9me3 is accompanied by a reduced Pol II occupancy at the target promoters suggests regulation of Pol II function by spLsd1/2 in mediating transcriptional activation. In recent reports, profiling of H3K9me2 and spLsd1/2 in the genome of *S. pombe* has detected enrichment in heterochromatin and euchromatin, respectively, in patterns that are broadly comparable to the ones reported here (Cam et al., 2005; Nicolas et al., 2006). However, the presence of methylated H3K9 in euchromatic regions, and of spLsd1 at heterochromatin boundaries, as well as a role for spLsd1 in regulating heterochromatin propagation and euchromatic gene transcription by antagonizing H3K9 methylation as an H3K9 demethylase, was not detected (Nicolas et al., 2006).

spLsd1/2 and Histone Demethylation

We were able to show that spLsd1 demethylates H3K9me2 using radioactively labeled bulk histones (Figure 2B). However, we were unable to detect demethylation by the highly sensitive mass spectrometry method (Whetstine et al., 2006) using methylated histone peptides, suggesting that spLsd1 may not be active toward peptide substrates. We were also unable to detect demethylation of nonradioactive bulk histones by measuring demethylation using modification-specific antibodies. It is possible that western blot may not be sensitive enough to detect low levels of demethylation as measured by a reduction of the methylation signal. In both cases, we used recombinant spLsd1 purified from bacteria and insect cells or spLsd1 protein complex from *S. pombe*. This suggests that spLsd1-mediated demethylation reaction was relatively inefficient in the in vitro assays, raising the question of whether the enzymatic activity is regulated. It is also interesting to note that spLsd1 displays H3K9, but not H3K4 demethylase activity, consistent with the observation that it acts primarily as a transcriptional activator in *S. pombe*. In contrast, the promoters of those genes that appeared to be repressed by spLsd1 are not bound by spLsd1, suggesting that they are indirect targets of spLsd1.

Human LSD1, through its "tower" domain (Yang et al., 2006), interacts with the SANT domain-containing

Co-REST for H3K4 demethylation and transcriptional repression. Unlike LSD1, spLsd1/2 do not have the tower domain and are not associated with any SANT domain-containing proteins, consistent with the fact that spLsd1 is an H3K9 rather than H3K4 demethylase, and that its primary function is activation and not repression. Human LSD1 can also function as H3K9 but only in the presence of the AR (Metzger et al., 2005). Moreover, a recent genome-wide localization study in human MCF7 cells also identified a general activator role of LSD1 at ERα-target promoters in a ligand-dependent manner, which is in part through its H3K9 demethylase activity (Garcia-Bassets et al., 2007). Thus, further investigation of the spLsd1 H3K9 substrate specificity will provide valuable insights into the dual specificity of human LSD1.

In sum, our studies demonstrated that spLsd1/2 regulate both heterochromatin expansion and euchromatic gene transcription in *S. pombe* in part by antagonizing H3K9 methylation through the H3K9 demethylase activity. In addition, a number of genes and noncoding RNA were upregulated rather than downregulated in the *lsd1* mutant. These genes are almost certainly indirect targets, as spLsd1 was not associated with them by ChIP-chip, but were also upregulated in the histone deacetylase double mutant *clr3Δ clr6-1* (Hansen et al., 2005). This suggests that spLsd1 may interact genetically with histone deacetylases, much like human LSD1, which physically and functionally interacts with histone deacetylases for repression in mammalian cells (Shi et al., 2005, Lee et al., 2006). The attenuated phenotype of the catalytic *lsd1* mutant in *S. pombe* and partial genetic suppression by *clr4Δ* also suggested that Lsd1/2 is likely to involve functions independent of the putative H3K9 demethylase activity, and these functions could include histone deacetylation. Misregulation of spLsd1/2 is expected to cause heterochromatin defects thereby impacting the epigenetic state of the cell. These findings provided significant insights into spLsd1/2 function, which may have important implications in understanding this important family of demethylases in other species.

EXPERIMENTAL PROCEDURES

Strain Construction

Strains with deletion of *splsd1*, point mutations in *splsd1* and *splsd2*, C-terminal TAP-tagged spLsd1, spLsd2, Phf1, and Phf2, and *pnmt81-splsd1* and *-splsd2* were generated by using a PCR-based module method (Bahler et al., 1998).

ChIP Analysis

S. pombe cells were fixed by 1% formaldehyde for 30 min at 30°C and quenched by 125 mM glycine for 5 min at room temperature. ChIP experiments were carried out as previously described (Verdel et al., 2004) by using antibodies against Swi6 (Abcam, 14898-100), mono-, di-, and trimethylated H3K9 (Upstate 07-450, 09-441, 09-442), and IgG-Sepharose beads (GE Healthcare). Genome-wide mapping of spLsd1, spLsd2, H3K4me2 (Upstate, 07-030), and H3K9me2 was performed according to manufactory instruction (Nimblegen). Sequences of the primers used in conventional ChIP assays were listed in Table S5. Conventional ChIP results were presented as the means with standard deviations from three independent experiments.

For ChIP analysis in Figures 2A, 3C, and 3D, we used multiplex PCR approach. Briefly, oligo pairs of the test regions were mixed with reference oligo pairs, which were chosen from euchromatic regions that show no transcriptional change in the *splsd1* mutant. The absolute signal levels of the experimental as well as the control may vary from experiments to experiments and are dependent on the amount of input material. However, the ratio of the control and the experimental signal should remain relatively constant, since these two PCR reactions occur in the same test tube. Two microliters out of 100 μl recovered ChIP DNA was used for each PCR reaction. Semiquantitative analyses were achieved by using ^{32}P-dCTP incorporation during amplification, and intensities of amplicons were acquired by phosphor image screen and ImageQuant TL program (Amersham Biosciences). Relative folds of enrichment were calculated as (test-IP/reference-IP)/(test-whole-cell extract [WCE]/reference-WCE). For ChIP analysis in Figures 5C and 5E, we used single pairs of oligos in PCR reactions with ^{32}P-dCTP incorporation, and the results were presented as percentage of WCE. The multiplex approach was not used because of the high H3K9me enrichment at heterochromatin boundaries, which resulted in a relative low level of amplification of the reference amplicon, making the internal reference less reliable.

Microarray Design and Hybridization

A whole-genome tiling array was implemented using a total of distinct 191,581 55-mer tiles with 65 bp spacing, designed using the forward strand of 2003 *S. pombe* genome assembly. No T_m matching was performed. Each spot was replicated twice on the array, and random GC content probes were included for quality control purposes. The array platform design can be found at the Gene Expression Omnibus (GEO) at NCBI as array platform GPL4749.

The ChIP samples and input DNA were prepared for microarray analysis by random amplification as described (Lippman et al., 2005). Reference designs including dye reversal were used to examine spLsd1, spLsd2, WT versus *splsd1Δ* H3K4me2, and WT versus *splsd1Δ* H3K9me2. Briefly, 7 μl of the immunoprecipitated DNA or a 1/100 dilution of input DNA was subjected to two rounds of sequenase primer extension with primer A, and later PCR amplified for 40 cycles with primer B. The PCR product was purified and concentrated to 0.5 μg/μl. Labeling, hybridization, and primary quantification were performed using the previously described microarray platform by Nimblegen.

RT-PCR and Expression Microarray

A reference design including dye reversal was used to examine genome-wide expression in *splsd1Δ* compared to WT. Total RNA from cells cultured to OD_{600} at 1.2 was isolated by hot acidic phenol and further purified by Absolutely RNA Miniprep Kit (Stratagene). For RT-PCR, cDNA was synthesized by using random N9 primer. For microarray hybridization, cDNA was produced from 10 μg of total RNA using the Superscript II Double-Stranded cDNA Synthesis Kit (Invitrogen) and oligo dT primer. Labeling, hybridization, and primary quantification were performed by Nimblegen.

Analysis of Microarray Data

Nimblegen-supplied data files were imported into the Bioconductor computing environment (http://bioconductor.org/). After performing quantile normalization, genotype-dependent transcriptional effects and ChIP enrichments were estimated for each probe by fitting a fixed linear model accounting for array, dye, and genotype effects to the data using the limma package (Smyth, 2004). Moderated t statistics and the log-odds score for differential expression or ChIP enrichment were computed by empirical Bayes shrinkage of the standard errors with the false discovery rate controlled to 0.05. Results of these computations were loaded into a relational MySQL database for subsequent positional analyses and also into a customized version of the

Generic Genome Browser, which is available for public inspection at http://chromatin.cshl.edu/demethylases/. Files containing per-probe signal estimates are available for public access at http://chromatin.cshl.edu/supplemental_data/demethylases/. In addition, raw microarray data have been deposited at NCBI GEO as series GSE6753.

To examine the physical distribution of spLsd1 and spLsd2 relative to transcriptional units, genes were divided into thirds. Promoters were considered to span the transcription start site to 500 bp upstream or the end of the closest gene, whichever was smallest. Average ChIP enrichment values were calculated over the promoter region and the segments of each gene. Per-gene transcriptional response in *splsd1Δ* was computed as an average of all probes within the transcriptional unit. Genes with average log2(fold) promoter enrichment for spLsd1 and/or spLsd2 ≥ 2 were considered to be major spLsd targets. Exploratory hierarchical and k-means clustering was performed on expression and spLsd1/2 distribution profiles using TIGR Multiple Experiment Viewer software (http://www.tm4.org/).

Complex Purification and Mass Spectrometry

A total of 5×10^{10} cells were used in each TAP purification as described previously (Verdel et al., 2004). Whole protein mixtures were digested in solution and analyzed by LC-MS/MS. Peptides were separated and on-line analyzed on a LTQ-FT hybrid mass spectrometer (ThermoElectron, San Jose, CA). Peptide matches were filtered to <0.5% false positives using a target-decoy database strategy. Final lists of proteins involved in the various complexes were obtained by subtracting protein matches found also in an untagged control sample.

Demethylation Assay and Mass Spectrometry

All histone substrates were radioactively labeled by GST-SET7/9 and GST-Clr4 purified from bacteria. Equal counts of the labeled substrates were used in histone demethylation reactions in the presence of recombinant Flag-spLsd1 purified from insect cells or the endogenous spLsd1 complex (Tsukada et al., 2006). Mass spectrometry analysis of the reaction products was described previously (Whetstine et al., 2006).

Reporter Assay

To monitor $Ade6^+$ expression, fresh colonies after growing on rich medium for 3 days (YEA) were streaked on EMM medium with low concentration of adenine (10 mg/l). Plates were incubated at 32°C for 3 days.

Supplemental Data

Supplemental Data include three figures, five tables, and Supplemental References and can be found with this article online at http://www.molecule.org/cgi/content/full/26/1/89/DC1/.

ACKNOWLEDGMENTS

We thank Stephen Buratowski for the Pol II antibody and Yota Murakami for helpful discussion. This work was supported by postdoctoral fellowships from the Spanish Ministry of Education and Science (M.Z. and J.V.) and by grants from the NIH to R.A.M. (GM067014) and to Yang Shi. (NCI118487).

Received: October 4, 2006
Revised: December 19, 2006
Accepted: February 22, 2007
Published: April 12, 2007

REFERENCES

Bahler, J., Wu, J.Q., Longtine, M.S., Shah, N.G., McKenzie, A., III, Steever, A.B., Wach, A., Philippsen, P., and Pringle, J.R. (1998). Heterologous modules for efficient and versatile PCR-based gene targeting in Schizosaccharomyces pombe. Yeast *14*, 943–951.

Bannister, A.J., and Kouzarides, T. (2004). Histone methylation: recognizing the methyl mark. Methods Enzymol. *376*, 269–288.

Cam, H.P., Sugiyama, T., Chen, E.S., Chen, X., FitzGerald, P.C., and Grewal, S.I. (2005). Comprehensive analysis of heterochromatin- and RNAi-mediated epigenetic control of the fission yeast genome. Nat. Genet. *37*, 809–819.

Fischle, W., Wang, Y., and Allis, C.D. (2003). Histone and chromatin cross-talk. Curr. Opin. Cell Biol. *15*, 172–183.

Garcia-Bassets, I., Kwon, Y.S., Telese, F., Prefontaine, G.G., Hutt, K.R., Cheng, C.S., Ju, B.G., Ohgi, K.A., Wang, J., Escoubet-Lozach, L., et al. (2007). Histone methylation-dependent mechanisms impose ligand dependency for gene activation by nuclear receptors. Cell *128*, 505–518.

Grewal, S.I. (2000). Transcriptional silencing in fission yeast. J. Cell. Physiol. *184*, 311–318.

Hall, I.M., Shankaranarayana, G.D., Noma, K., Ayoub, N., Cohen, A., and Grewal, S.I. (2002). Establishment and maintenance of a heterochromatin domain. Science *297*, 2232–2237.

Hansen, K.R., Burns, G., Mata, J., Volpe, T.A., Martienssen, R.A., Bahler, J., and Thon, G. (2005). Global effects on gene expression in fission yeast by silencing and RNA interference machineries. Mol. Cell. Biol. *25*, 590–601.

Irvine, D.V., Zaratiegui, M., Tolia, N.H., Goto, D.B., Chitwood, D.H., Vaughn, M.W., Joshua-Tor, L., and Martienssen, R.A. (2006). Argonaute slicing is required for heterochromatic silencing and spreading. Science *313*, 1134–1137.

Ivanova, A.V., Bonaduce, M.J., Ivanov, S.V., and Klar, A.J. (1998). The chromo and SET domains of the Clr4 protein are essential for silencing in fission yeast. Nat. Genet. *19*, 192–195.

Kouzarides, T. (2002). Histone methylation in transcriptional control. Curr. Opin. Genet. Dev. *12*, 198–209.

Lachner, M., Sengupta, R., Schotta, G., and Jenuwein, T. (2004). Trilogies of histone lysine methylation as spigenetic landmarks of the eukaryotic genome. Cold Spring Harb. Symp. Quant. Biol. *69*, 209–218.

Lee, M.G., Wynder, C., Cooch, N., and Shiekhattar, R. (2005). An essential role for CoREST in nucleosomal histone 3 lysine 4 demethylation. Nature *437*, 432–435.

Lee, M.G., Wynder, C., Bochar, D.A., Hakimi, M.A., Cooch, H., and Shiekhattar, R. (2006). Functional interplay between histone demethylase and deacetylase enzymes. Mol. Cell. Biol. *26*, 6395–6402.

Lehnertz, B., Ueda, Y., Derijck, A.A., Braunschweig, U., Perez-Burgos, L., Kubicek, S., Chen, T., Li, E., Jenuwein, T., and Peters, A.H. (2003). Suv39h-mediated histone H3 lysine 9 methylation directs DNA methylation to major satellite repeats at pericentric heterochromatin. Curr. Biol. *13*, 1192–1200.

Lippman, Z., Gendrel, A.V., Colot, V., and Martienssen, R. (2005). Profiling DNA methylation patterns using genomic tiling microarrays. Nat. Methods *2*, 219–224.

Margueron, R., Trojer, P., and Reinberg, D. (2005). The key to development: interpreting the histone code? Curr. Opin. Genet. Dev. *15*, 163–176.

Martienssen, R.A., Zaratiegui, M., and Goto, D.B. (2005). RNA interference and heterochromatin in the fission yeast Schizosaccharomyces pombe. Trends Genet. *21*, 450–456.

Martin, C., and Zhang, Y. (2005). The diverse functions of histone lysine methylation. Nat. Rev. Mol. Cell Biol. *6*, 838–849.

Mata, J., Lyne, R., Burns, G., and Bahler, J. (2002). The transcriptional program of meiosis and sporulation in fission yeast. Nat. Genet. *32*, 143–147.

Metzger, E., Wissmann, M., Yin, N., Muller, J.M., Schneider, R., Peters, A.H., Gunther, T., Buettner, R., and Schule, R. (2005). LSD1 demethylates repressive histone marks to promote androgen-receptor-dependent transcription. Nature *437*, 436–439.

Nakayama, J.-I., Rice, J.C., Strahl, B.D., Allis, C.D., and Grewal, S.I.S. (2001). Role of histone H3 lysine 9 methylation in epigenetic control of heterochromatin assembly. Science *292*, 110–113.

Nicolas, E., Lee, M.G., Hakimi, M.A., Cam, H., Grewal, S.S., and Shiekhattar, R. (2006). Fission yeast homologs of human histone H3 lysine 4 demethylase regulate a common set of genes with diverse functions. J. Biol. Chem. *281*, 35983–35988.

Noma, K., Allis, C.D., and Grewal, S.I. (2001). Transitions in distinct histone H3 methylation patterns at the heterochromatin domain boundaries. Science *293*, 1150–1155.

Noma, K., Cam, H.P., Maraia, R.J., and Grewal, S.I. (2006). A role for TFIIIC transcription factor complex in genome organization. Cell *125*, 859–872.

Peters, A.H., O'Carroll, D., Scherthan, H., Mechtler, K., Sauer, S., Schofer, C., Weipoltshammer, K., Pagani, M., Lachner, M., Kohlmaier, A., et al. (2001). Loss of the Suv39h histone methyltransferases impairs mammalian heterochromatin and genome stability. Cell *107*, 323–337.

Pidoux, A.L., and Allshire, R.C. (2004). Kinetochore and heterochromatin domains of the fission yeast centromere. Chromosome Res. *12*, 521–534.

Rea, S., Eisenhaber, F., O'Carroll, D., Strahl, B.D., Sun, Z.-W., Schmid, M., Opravil, S., Mechtler, K., Ponting, C.P., Allis, C.D., and Jenuwein, T. (2000). Regulation of chromatin structure by site-specific histone H3 methyltransferases. Nature *406*, 593–599.

Sanders, S.L., Portoso, M., Mata, J., Bahler, J., Allshire, R.C., and Kouzarides, T. (2004). Methylation of histone H4 lysine 20 controls recruitment of Crb2 to sites of DNA damage. Cell *119*, 603–614.

Scott, K.C., Merrett, S.L., and Willard, H.F. (2006). A heterochromatin barrier partitions the fission yeast centromere into discrete chromatin domains. Curr. Biol. *16*, 119–129.

Shankaranarayana, G.D., Motamedi, M.R., Moazed, D., and Grewal, S.I. (2003). Sir2 regulates histone H3 lysine 9 methylation and heterochromatin assembly in fission yeast. Curr. Biol. *13*, 1240–1246.

Shi, Y., Lan, F., Matson, C., Mulligan, P., Whetstine, J.R., Cole, P.A., Casero, R.A., and Shi, Y. (2004). Histone demethylation mediated by the nuclear amine oxidase homolog LSD1. Cell *119*, 941–953.

Shi, Y.J., Matson, C., Lan, F., Iwase, S., Baba, T., and Shi, Y. (2005). Regulation of LSD1 histone demethylase activity by its associated factors. Mol. Cell *19*, 857–864.

Smyth, G.K. (2004). Linear models and empirical bayes methods for assessing differential expression in microarray experiments. Stat. Appl. Genet. Mol. Biol. *3*, Article 3.

Tsukada, Y., Fang, J., Erdjument-Bromage, H., Warren, M.E., Borchers, C.H., Tempst, P., and Zhang, Y. (2006). Histone demethylation by a family of JmjC domain-containing proteins. Nature *439*, 811–816.

Vakoc, C.R., Mandat, S.A., Olenchock, B.A., and Blobel, G.A. (2005). Histone H3 lysine 9 methylation and HP1gamma are associated with transcription elongation through mammalian chromatin. Mol. Cell *19*, 381–391.

Verdel, A., Jia, S., Gerber, S., Sugiyama, T., Gygi, S., Grewal, S.I., and Moazed, D. (2004). RNAi-mediated targeting of heterochromatin by the RITS complex. Science *303*, 672–676.

Volpe, T.A., Kidner, C., Hall, I.M., Teng, G., Grewal, S.I., and Martienssen, R.A. (2002). Regulation of heterochromatic silencing and histone H3 lysine-9 methylation by RNAi. Science *297*, 1833–1837.

Whetstine, J.R., Nottke, A., Lan, F., Huarte, M., Smolikov, S., Chen, Z., Spooner, E., Li, E., Zhang, G., Colaiacovo, M., and Shi, Y. (2006). Reversal of histone lysine trimethylation by the JMJD2 family of histone demethylases. Cell *125*, 467–481.

Yang, M., Gocke, C.B., Luo, X., Borek, D., Tomchick, D.R., Machius, M., Otwinowski, Z., and Yu, H. (2006). Structural basis for CoREST-dependent demethylation of nucleosomes by the human LSD1 histone demethylase. Mol. Cell *23*, 377–387.